applied sciences

MDPI

Article

Robustness of Model-Predictive and Passivity-Based Control in the Three-Phase DC/AC Converter Application

Łukasz Dyga [1], Mohammed Alhasheem [2,*], Pooya Davari [3] and Zbigniew Rymarski [1]

[1] Department of Electronics, Electrical Engineering and Microelectronics, Faculty of Automatic Control, Electronics and Computer Science, Silesian University of Technology, Akademicka 16, 44-100 Gliwice, Poland; lukasz.dyga@polsl.pl (Ł.D.); zbigniew.rymarski@polsl.pl (Z.R.)

[2] Electrical and Control Department, Arab Academy for Science, Technology and Maritime Transport, Cairo 2033, Egypt

[3] Department of Energy Technology, Aalborg University, Pontoppidanstræde 101, 2-051, 9220 Aalborg, Denmark; pda@energy.aau.dk

* Correspondence: m.a.hasheem@aast.edu

Abstract: In modern controller design, various solutions for controlling power converter systems can be found depending on their applications, speed of working, pulse width modulation (PWM) techniques, switching frequencies—f_c, and different load types. The need to manipulate control parameters can be often observed in classical structures, e.g., well-known PID, repetitive, or deadbeat control particularly sensitive to distinct parameters uncertainties. The purpose of this paper is to present an improved version of controllers designated for a UPS that will be considerably resistant to model changes. Proposed control techniques are independent of unexpected output filter changes: L_f—filter coil inductance and C_f—filter capacitor conductance. The second aspect of this paper is to compare effectiveness of modified predictive MPC (model-predictive control) and feedback PBC (passivity-based control) controllers in reducing output voltage total harmonic distortion (THD) for various load values. The biggest distortions of output voltage were observed during experiments with nonlinear RC load. Both simulation and experimental verification of mismatching parameters were performed and examined. Thanks to the proposed solution, the output voltage THD_v quality factor was reduced below 8% in an efficient way for all the applied loads and stayed at the level of 1% when well-matched filter parameters were provided.

Keywords: DC/AC converter; PBC; MPC; robustness; uninterruptible power supply (UPS); power converters; inverters; control algorithms

check for updates

Citation: Dyga, Ł.; Alhasheem, M.; Davari, P.; Rymarski, Z. Robustness of Model-Predictive and Passivity-Based Control in the Three-Phase DC/AC Converter Application. *Appl. Sci.* **2022**, *12*, 4329. https://doi.org/10.3390/app12094329

Academic Editor: Rodolfo Dufo-López

Received: 2 April 2022
Accepted: 22 April 2022
Published: 25 April 2022

1. Introduction

Typical modern feedback or predictive controllers are single-input single-output (SISO) or multiple-input single-output (MISO) controllers [1,2]. In case of the MISO controller in DC/AC converter, an application system analyzes three main input variables [3,4]. Those are output voltage—v_o, output current—i_o, and filter current—i_{lf}. On the other hand, the simplest SISO control method is based only on the output voltage. The main advantage of application of the MISO controller is the effective control functionality and reducing output voltage THD_v [5,6]. Moreover, we should observe a faster outcome of the steady state and lower voltage overshoot for the dynamic load type in comparison with the SISO control mode.

Multiple-input control in the early stage of working is much more effective than other solutions. It provides reduction of different distortions, mainly skewness and unbalancing phenomenon [7]. On the other hand, this type of control is much more burdensome for CPU processing power, which is often limited due to the number of calculations and delays that could occur in an experimental system. That was observed during three-phase Clarke or Park transformation and its reverse transformation for each of the control variables performed simultaneously. It must be also distinguished that the harmonics higher than $f_c/2$ are compensated by the previously implemented LC output filter for the standalone inverter device [7,8].

The designing process of the DC/AC converter should start with designing the LC filter (proper C_f and L_f material selection) and calculating its values [9]. This procedure has a significant influence on the quality of the output voltage v_o [9,10]. Nonetheless, switching frequency f_c value also has a big impact on the control and system stability. Divergence from the previously calculated LC values may occur in the system due to many reasons: electronic component damage or poor quality of manufacturer's design. However, the designed controller should be able to decrease the values of the output distortion according to the applicable standards, e.g., IEC 61000-2-2, EN 62040-3, and IEEE 519-2014 [11–13]. Lower harmonics must be reduced by the feedback control loop or by prediction of the state variables. They are typically implemented in stationary $\alpha\beta$ or dq rotating reference frame in accordance with the three-phase topology and potential necessity of decoupling application.

The motivation behind this paper is to show advantages and disadvantages of the proposed improved controllers dedicated especially for the DC/AC standalone inverters in UPS application [4]. The robustness of the system with an output filter provided with mismatching parameters is highlighted in this study for two forms of MISO control: feedback tracking system with a modulator and state variable prediction without using a modulator. The goal is to discriminate between the two control systems based on two critical performance metrics and recommend the best operation using either passivity or predictive methods.

In this context, especially in terms of controller design, it is preferable to choose a method that allows for a flexible design capable of addressing the issue of having fewer control inputs than control variables while maintaining system stability. Passivity-based control approaches [1,2] provide for a methodical approach to controller design, with the system structure clearly defined. Interconnection and damping assignment (IDA) is one of these strategies. It entails selecting a desirable closed-loop energy function and ensuring that the control error converges to zero. Furthermore, determining controller parameters is, to some extent, easier than in other procedures. For these reasons, IDA-based controllers for various power converters, such as rectifiers and inverters, have already been improved and presented here.

Finite-control-set model-predictive control (FCS-MPC), on the other hand, has become a prominent technique for power converter control [7]. It is built on the premise of employing a discrete VSC model with accompanying filter to forecast future behavior for all potential control inputs, and then applying the one that minimizes a programmed cost function (CF) at each sampling time [9]. This technique has been widely and effectively applied to standalone converters due to its flexibility and intrinsically fast reaction. The online evaluation of all conceivable switch configurations can be performed over many periods, but the number of computations grows exponentially with each step. In this research, an improved algorithm is presented and compared to the enhanced passivity model.

The system design overview for the 2L-VSI will be discussed in Section 2, while the improved passivity-based control will be discussed in Section 3 and the improved model predictive control will be discussed in Section 4. The simulation results and discussion are given in Section 5 and the experimental validations are given in Section 6, while the discussion is reported in Section 7 and conclusions in Section 8.

2. System Design Overview

The three-phase inverter used during investigations is shown in Figure 1. Comparison of the presented solutions is made using both MATLAB simulation and experimental verification. The switching frequency f_c was set to 12.8 kHz—due to utilized hardware components, such as Matlab dSPACE device boards: dSPACE controller, DS5101 and DS2004 A/D, and inverter Danfoss 131F3040, used in empirical tests. The important fact that should be highlighted is that the PBC controller was working with the constant switching frequency and used the f_c as one of its input values in the control law. On the other hand, the MPC algorithm was using an average switching frequency calculated by the cost function J in the currently used operating sector vector depending on the sampling time [14,15]. In the MPC controller, the PWM modulator and the control functions calculations are merged into one state, whereas in the PBC controller the modulator is located at the output of the control function. This fact leads to the assumption that operating frequency was set to 12.8 kHz in order to have a fair comparison between feedback PBC and predictive MPC [16,17]. Typical load types for standalone systems are mainly static-resistive R, dynamic R, and nonlinear rectified RC load. Additionally, the initial values of L_f = 3 mH and C_f = 60 µF were taken into calculation during simulation. The paper presents a methodology of designing, implementation, and verification of the two types of MISO controllers—MPC and PBC—with their improved modifications of the control function. Thus, the calculations are based on $\alpha\beta$ transformation. Both of the controllers used the same input variables, output filter values, and were working in the same stress condition—constant input DC voltage—600 V and changeable L_f and C_f values. The installation configuration is presented in Figure 1, and basic parameters of the studied system are listed in Table 1.

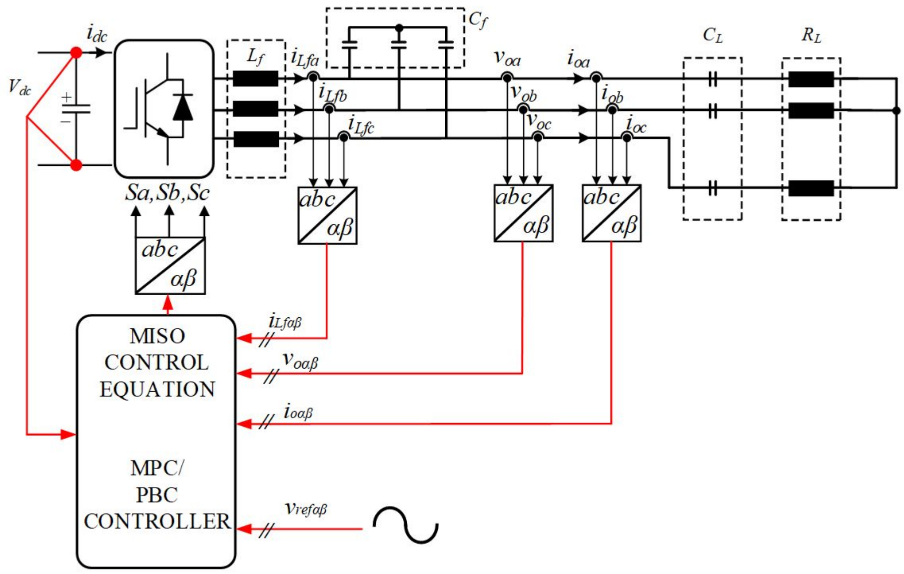

Figure 1. Control schematic for MPC/PBC controller with the RC load type.

Table 1. Parameters of the studied experimental system.

Parameter	Symbol	Value
DC link voltage	V_{dc}	600 V
Switching frequency	f_c	12,800 Hz
Nonlinear load (diode rectifier)	C_L, R_L	460 µF, 35 Ω
Sampling time	T_s	39 µs
Nominal RMS output voltage (L-L)	$v_{o,ref}$	173 V
Reference wave frequency	f_{ref}	50 Hz

3. Improved Passivity-Based Control

At the beginning of investigation for that type of control, the object (three-phase inverter) should be described using Euler–Lagrange equations or Port-Hamiltonian energy conversion system analysis [18]. The PCH model ensures interconnection structure related to energy shaping, so it is more beneficial for the PBC controller. In case of passivity control we are focusing on different rules for energy shaping [19,20]. The examined system will be also further referred to as Port-Hamiltonian type. The simplest case of PBC conventional algorithm is based on the linearization of the system equation and its Lagrangian, which is not the purpose of this paper. The IPBC2-used controller is based on IDA-PBC methodology, which consists of the desired interconnections and damping matrices [21]. The next stage is solving the partial differential equation (PDE). The PBC control is the sum of total energy shaping and additionally assumed damping. This type of control is designated for all systems that could store energy on their elements—a typical feedback system that could use energy shaping principle. In the first step, the number of phases should be identified and internal structure of the bridge analyzed—in this case, H type full bridge 2L-VSI. This allows indicating the coefficient of the components in the input matrix. In the next step, based on the equations for each phase, the natural energy must be changed via adding additional resistance R_i, named dissipative factor. The controller should track the reference error of the state variable x. The process was first mentioned by Ortega [1]. The system is very often represented in the dq rotationary frame. For investigation, an improvement of the IDA-PBC [22,23] method was investigated—IPBC2 presented in [24], but based on the non-interconnection equations in the matrix J. In that solution, the controlled variables were introduced to the stationary $\alpha\beta$ frame. This is connected to the fact that $\alpha\beta$ leads to obtaining additional derivative factor over the capacitor variable. The only tunable parameters are voltage gain and dissipation factor. That additional tracking affects K_v, which is the gain of the output voltage included in the control of each phase. In the calculation it depends on switching frequency, because of the occurrence of the derivatives. This type of control was previously used in other papers, e.g., with the dynamic resistive R load during the unbalanced defects in the delta connected inverter. The system should be described in the abc rotationary frame, taking into account the coefficient depending on the load type, star or delta, and the modulation technique [16,21]. In this study, the star load connection was implemented both for MPC and PBC. The internal matrix coefficients for the Clarke transformation vary in case of the used load type [16]. The load current is treated as an independent disturbance. In case of application of the passivity-based control, the system must fulfill two conditions [1,19]:

- System without the feedback must be stable.
- Stored energy must be lower than supplied energy.

The problem formulation comes down to description of the system by the following Equations (1) and (2). The IPBC2 problem formulations focused on the difference between interconnection matrix and dissipation matrix and handling the error between current and previous states. Based on [21,24], the interconnection does not occur and J is just the identity matrix. $R(x)$ represents damping matrix, which is the sum of the R_{Lf} and dissipating resistance R_i, which is 10. $G(x)$ represents input matrix, where u is the input vector and ξ is the system disturbance. Input matrix is the DC voltage. During experiments, proper adjustment of the modulation index must be ensured. The system should prevent PWM modulator saturation due to the high-voltage gain response of the output control.

$$\dot{x} = [J(x) - R(x)]\frac{\partial H}{\partial x}(x) + g(x)u + \xi \tag{1}$$

The $H(x)$ represents total stored energy [18,20]; u and y are the input control vector and output voltage, respectively.

$$y = g^{\top}(x)\frac{\partial H}{\partial x}(x) + D(x)u \tag{2}$$

$$x_{\alpha\beta} = [i_{Lf\alpha\beta} \quad i_{o\alpha\beta} \quad v_{o\alpha\beta}] \tag{3}$$

$$y_{\alpha\beta} = [v_{o\alpha} \quad v_{o\beta}] \tag{4}$$

The total energy is represented by the Hamiltonian m external port system equation concerning LC circuits [1]. Hence, to the linear system consideration, Hamiltonian has a quadratic form.

$$H(x) = \frac{1}{2}x^{\top}Qx \tag{5}$$

The state variable could be then rewritten basing on the PH system including necessary interconnection and dissipation matrices $J_{\alpha\beta}$ and $R_{\alpha\beta}$ [1,19].

$$\dot{x}_{\alpha\beta} = [J_{\alpha\beta} + R_{\alpha\beta}]P^{-1}x_{\alpha\beta} + G_{\alpha\beta} + D_{\alpha\beta}d_{\alpha\beta} \tag{6}$$

$$A_{\alpha\beta} = \begin{bmatrix} -R_{Lf}/L_f & 0 & -1/L_f \\ 0 & 0 & 0 \\ 1/C_f & -1/C_f & 0 \end{bmatrix} \tag{7}$$

$$B_{\alpha,\beta} = \begin{bmatrix} 1/L_f \\ 0 \\ 0 \end{bmatrix}, \quad C_{\alpha,\beta} = \begin{bmatrix} 0 & 0 & 1 & 0 \end{bmatrix}. \tag{8}$$

$$R_{\alpha\beta} = \begin{bmatrix} R_i + R_{Lf} & 0 & 0 & 0 \\ 0 & R_i + R_{Lf} & 0 & 0 \\ 0 & 0 & K_v & 0 \\ 0 & 0 & 0 & K_v \end{bmatrix} \tag{9}$$

$$P = \begin{bmatrix} L_f & 0 & 0 & 0 \\ 0 & L_f & 0 & 0 \\ 0 & 0 & C_f & 0 \\ 0 & 0 & 0 & C_f \end{bmatrix}, J_{\alpha\beta} = \begin{bmatrix} 0 & 0 & -1 & 0 \\ 0 & 0 & 0 & -1 \\ 1 & 0 & 0 & 0 \\ 0 & 1 & 0 & 0 \end{bmatrix} \tag{10}$$

$$G_{\alpha\beta} = \begin{bmatrix} V_{dc} & 0 \\ 0 & V_{dc} \\ 0 & 0 \\ 0 & 0 \\ 0 & 0 \end{bmatrix}, \quad D_{\alpha\beta} = \begin{bmatrix} 0 & 0 \\ 0 & 0 \\ -1 & 0 \\ 0 & -1 \end{bmatrix} \tag{11}$$

$$d_{\alpha\beta} = [i_{o\alpha\beta} \quad i_{o\alpha\beta}] \tag{12}$$

The total energy in the presented system is the overall sum of the energy stored in the output filters components [24].

$$\begin{aligned} G_{\alpha\beta,dq} = \frac{L_f di_{Lf\alpha\beta prev}}{dt} + R_{Lf}i_{L\alpha\beta prev} - \\ -R_i(i_{Lf\alpha\beta} - i_{Lf\alpha\beta prev}) + v_{o\alpha prev} \end{aligned} \tag{13}$$

For calculation of the IPBC2 controller [24], the value of the reference filter current is needed—$i_{L\alpha\beta prev}$. In this element, it is necessary to take into account the value of the difference between output and reference voltage, so the results should be more robust not only for the output filter current but also for the output filter voltage.

$$K_v(v_{o\alpha\beta} - v_{o\alpha\beta prev}) \tag{14}$$

The control law for the stationary $\alpha\beta$ frame for the $K_v = 0$ is the same as the one for the conventional PBC [25]. Introducing K_v (the control of the output voltage error) makes the control law IPBC version. The final form consists of the derivative over the output voltage and voltage gain—IPBC2. On the other hand, the derivative over the C_f makes the system stabilize even longer and it is an important factor in the process of decreasing the THD_v. During implementation, the system should behave passively. Parameters in Table 2 maintain stability and passiveness of control. The condition is to store energy less than or equal to the total supplied energy to the system [1]. Additionally, it must be taken into account that passive controllers could modify only destabilizing forces—the forces acting on the system are divided into stabilizing, destabilizing, and supporting ones [1].

Table 2. Control parameters of the IPBC2 controller, voltage gain—K_v, and additional input resistance factor—R_i.

Parameter	Value
K_v	2
R_i	10

4. Improved Model-Predictive Control

Electrical drivers, UPS, and grid-connected inverters have all been proposed as applications for MPC [26,27]. FCS-MPC is based on the principle of employing a discrete model of the power converter and its associated filter to anticipate future behavior for all potential control inputs and then applying the best one that minimizes a predetermined cost function (CF) at each sampling period. The main concept is to harness the microcontroller's raw processing capability to integrate all control loops in a single algorithm that takes into account the converter's model and accompanying filter. A three-phase voltage source inverter driven by the FCS-MPC is shown in Figure 1 as a general block diagram.

The method is conducted sequentially in its most basic form, and at the start of each sampling time (T_s), it applies new switching configurations generated based on the measurements from the previous step [7]. It then receives new and updated measurements in order to select new switching configurations. The three-phase 2L-VSI power circuit is considered, with the two switches in each leg operating in a complimentary mode [28,29]. The switching states can be represented by the switching signals S_{ka}, S_{kb}, and S_{kc}, which are defined as follows:

$$S_{ka} = \begin{cases} 1 \text{ if } S_1 \text{ on and } S_4 \text{ off} \\ 0 \text{ if } S_1 \text{ off and } S_4 \text{ on} \end{cases} \tag{15}$$

$$S_{kb} = \begin{cases} 1 \text{ if } S_2 \text{ on and } S_5 \text{ off} \\ 0 \text{ if } S_2 \text{ off and } S_5 \text{ on} \end{cases} \tag{16}$$

$$S_{kc} = \begin{cases} 1 \text{ if } S_3 \text{ on and } S_6 \text{ off} \\ 0 \text{ if } S_3 \text{ off and } S_6 \text{ on} \end{cases} \tag{17}$$

The filter inductance (L_{fa}, L_{fb}, L_{fc}) equation can be expressed in the vectorial form as

$$L_f \frac{\mathrm{d}i_{L_f}}{\mathrm{d}t} = v_i - v_o \tag{18}$$

where L_f is the filter inductance and i_{Lf} and v_o are the filter current and voltage, respectively. Variable v_i is the inverter voltage of the system, and it has eight different voltage vectors, as shown in Figure 2.

The equation that describes the dynamic behavior of the output voltage can be expressed as

$$C_f \frac{\mathrm{d}v_o}{\mathrm{d}t} = i_{L_f} - i_o \tag{19}$$

where C_f is the filter capacitance (C_{fa}, C_{fb}, C_{fc}) and i_o is the load current, which can be estimated or measured. These equations can be rewritten in the state space model as [30,31]:

$$\frac{\mathrm{d}X}{\mathrm{d}t} = AX + B_1 v_i + B_2 i_o \tag{20}$$

where,

$$X = \begin{bmatrix} i_{L_f} \\ v_o \end{bmatrix} \tag{21}$$

$$A = \begin{bmatrix} -R/L_f & -1/L_f \\ 1/C_f & 0 \end{bmatrix} \tag{22}$$

$$B_1 = \begin{bmatrix} 1/L_f \\ 0 \end{bmatrix} \tag{23}$$

$$B_2 = \begin{bmatrix} 0 \\ -1/C_f \end{bmatrix} \tag{24}$$

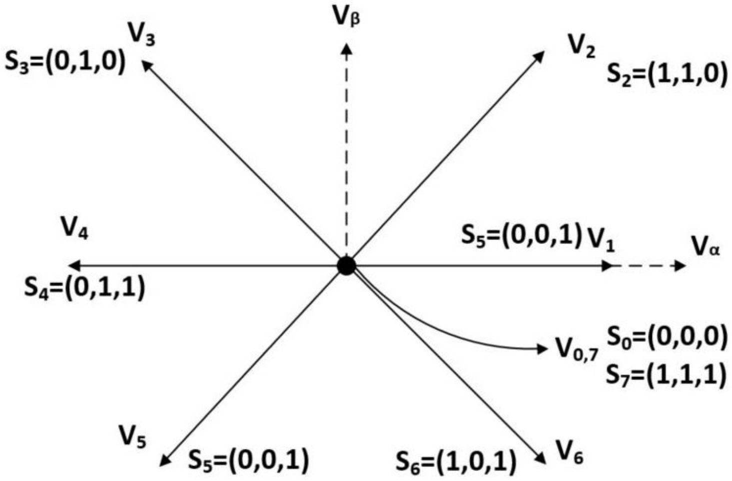

Figure 2. MPC controller vector states for 2L-VSI.

A discrete model is obtained from (20) and it can be expressed as follows:

$$x(k+1) = A_q x(k) + B_q v_i(k) + B_{dq} i_o(k) \tag{25}$$

where

$$A_q = exp^{AT_s} \tag{26}$$

$$B_q = \int_0^{T_s} exp^{A\tau} B_1 d\tau \tag{27}$$

$$B_{dq} = \int_0^{T_s} exp^{A\tau} B_2 d\tau. \tag{28}$$

This model is used to calculate the prediction of filter voltage and currents for every possible input voltage. The selection of the optimal output voltage vector depends on the evaluation of CF. The two different CFs for such system will be [30]:

$$J = (v^*_{o\alpha} - v^p_{o\alpha}(k+1))^2 + (v^*_{o\beta} - v^p_{o\beta}(k+1))^2 + (\lambda_d * g_I) \tag{29}$$

$$g_I = (i_{Lf\alpha} - i_{o\alpha} + C_f \omega_{ref}(v^*_{o\beta}))^2 + (i_{Lf\beta} - i_{o\beta} + C_f \omega_{ref}(v^*_{o\alpha}))^2 \tag{30}$$

where $\lambda_d = 0.6$.

5. Simulation Results

Figures 3–6 present the results for the Matlab simulation model output voltages for the nonlinear rectified RC load. The investigations were performed using the load capacitor—$C_L = 460$ µF to show the controller behavior for the higher load conditions. The value of the output filter capacitor was intentionally increased based on many papers, especially concerning PBC controllers $C_f = 60$ µF [21,22]. During simulations, the overall behavior of the system was examined, including time responses and delays. The figures show the third period due tuning both the controllers. In case of PBC, one period delay was observed in comparison to the MPC output voltage THD stabilization on some constant level. The simulations parameters are based on [24]; however, the system presented in this paper was tuned to the balanced load with changeable filter parameters to maintain the good output voltage quality. The system must fulfill, in the same time, the necessary stabilization conditions for both the controllers. Almost all the results are oscillating about 1% of the output voltage THD_v; the most harmful was decreasing the output filter coil.

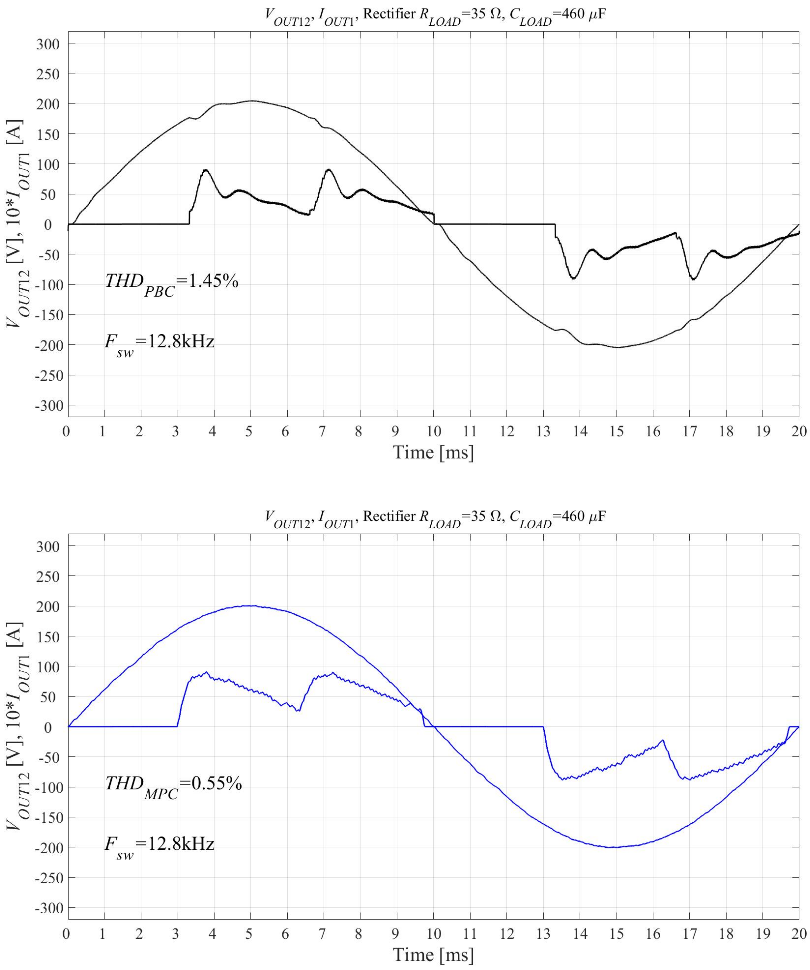

Figure 3. Mismatching the value of C_f—decreasing the initial value to 40 µF.

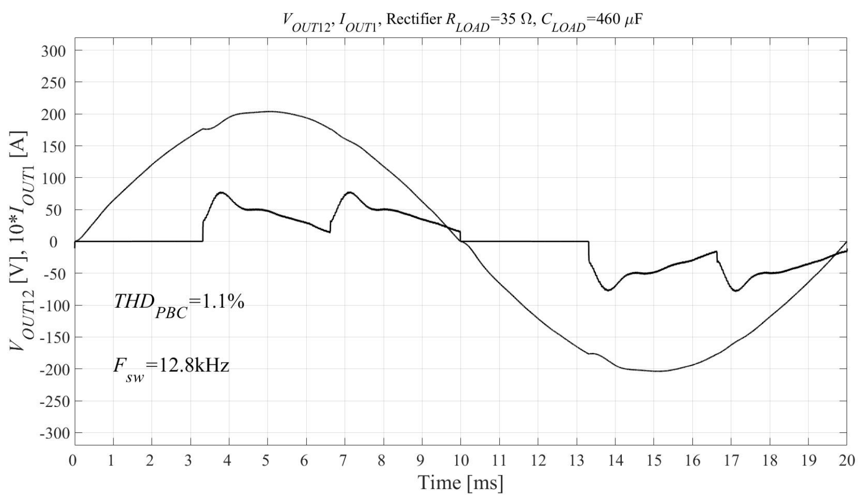

Figure 4. *Cont.*

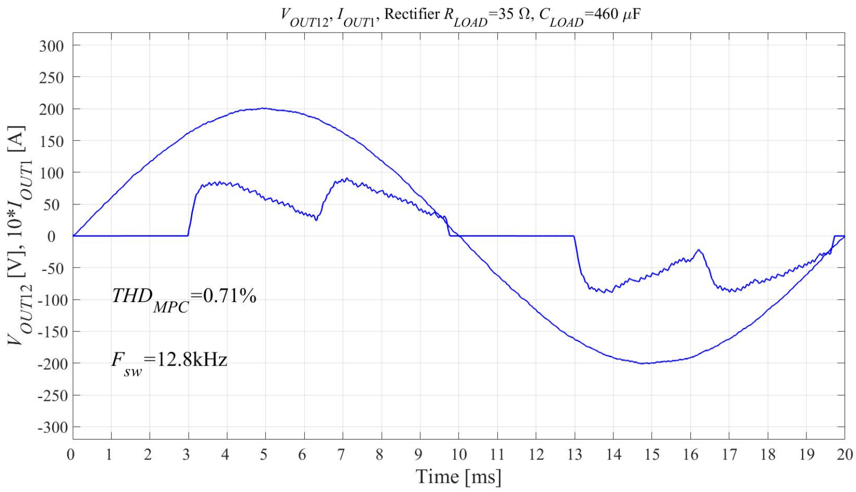

Figure 4. Mismatching the value of L_f—increasing the initial value to 4 mH.

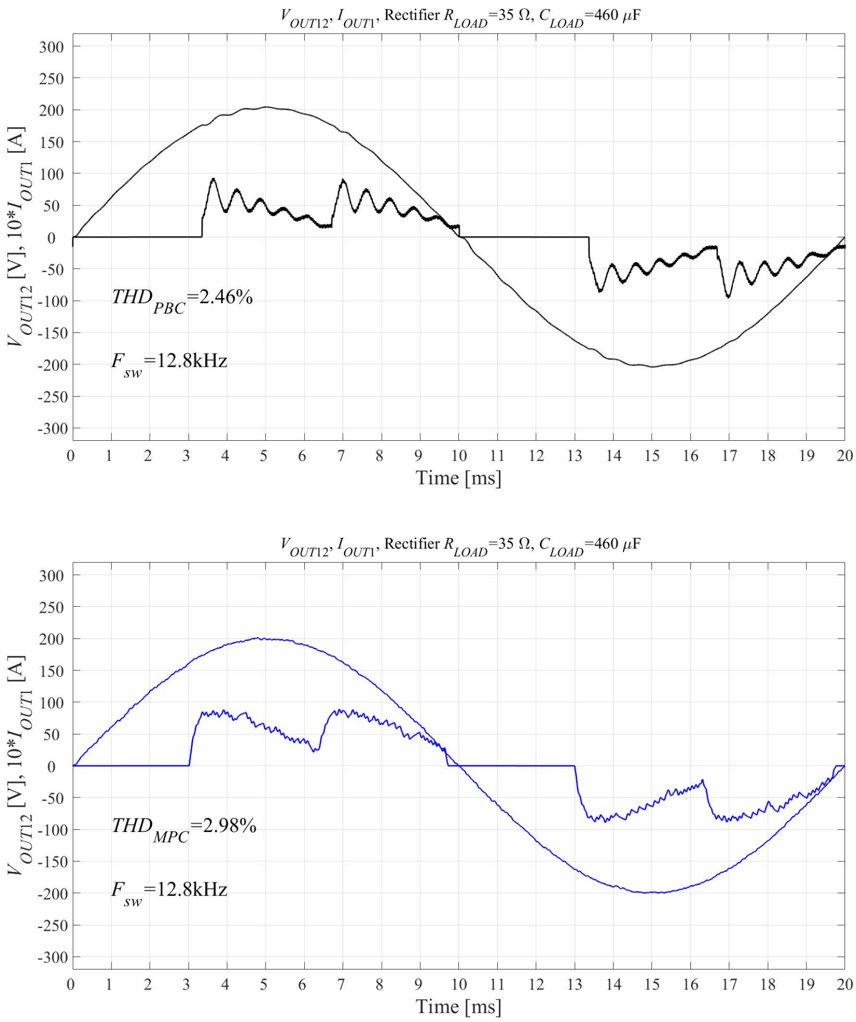

Figure 5. Mismatching the value of L_f—decreasing the initial value to 2 mH.

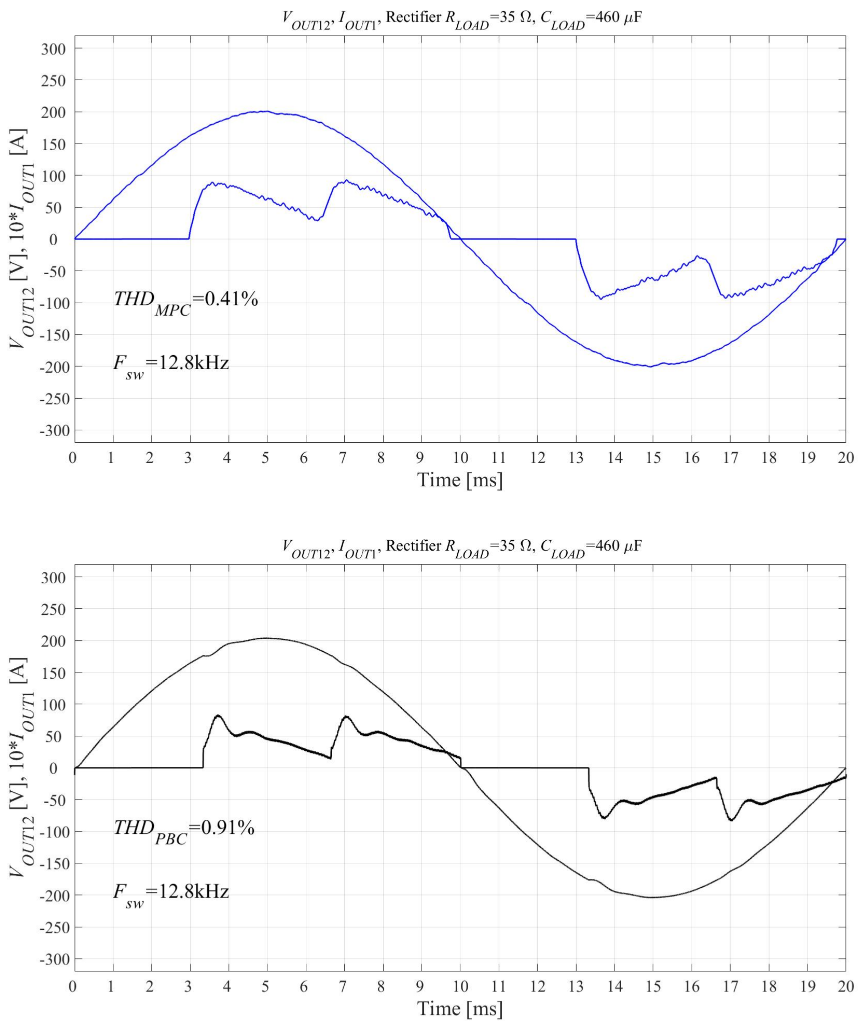

Figure 6. Output voltage for initial value of the output LC filter parameters $L_f = 3$ mH, C_f = 50 µF without mismatching.

6. Experimental Validation

The experimental verification assumed downgrading the value of C_f, moreover decreasing and increasing the value of the filter inductor. Values used in the presented experiment depended strictly on the manufacturer components. The values of L_f and C_f are presented in Table 3. Worse results were obtained for the output filter inductor decreasing. The MPC controller is oscillating on the border of the high-quality S classification according to the EN 62040-3 standard.

In addition, PBC output voltage THD rose to about 5%, the border of the IEEE 519-2014 standard. In Figures 7 and 8, the waveform is a good-quality sine wave, except for the low inductor mismatching case. PBC results in unbalancing between phases and MPC has the problem with the current prediction step to boost the current at the most skew segments of the output voltage. The following observations were made during the experiments (Figure 9). Decreasing values of the inductor filter seemed to considerably deteriorate system behavior. The advantages of increasing capacitor values incurred the risk of the output power factor (PF). Therefore, the capacitor value could not be increased infinitely, even though some power factor correction systems were additionally applied.

Table 3. THD_v % experimental results for different filter parameters for the nonlinear RC load: C_L = 460 µF, R_L = 35 Ω.

Filter Parameters	MPC Improved %	PBC Improved %
L_f = 3 mH, C_f = 60 µF initial	0.97	0.56
L_f = 2 mH, mismatch L_f	7.55	4.61
L_f = 4 mH mismatch L_f	0.67	1.06
C_f = 40 µF mismatch C_f	1.09	0.45

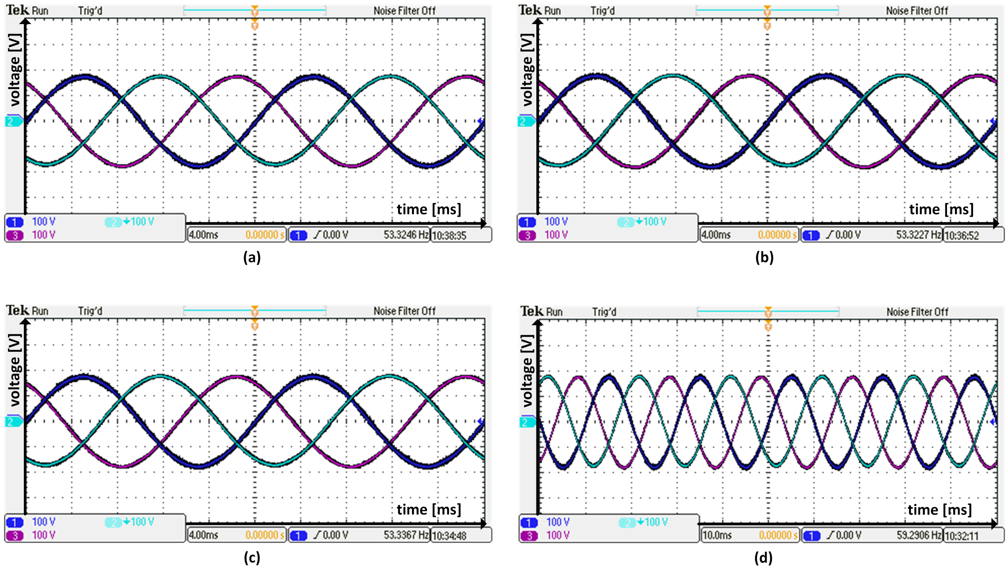

Figure 7. Output voltage IPBC2 for nonlinear RC load: (**a**) mismatching C_f = 40 µF, (**b**) mismatching $L_f = 2$ mH, (**c**) mismatching $L_f = 4$ mH, (**d**) normal work condition.

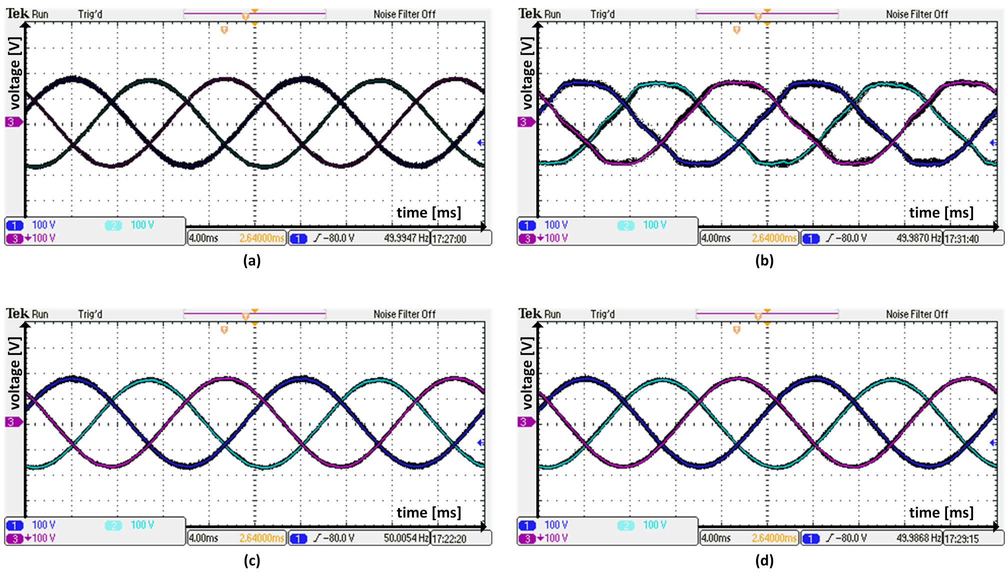

Figure 8. Output voltage MPC for nonlinear RC load: (**a**) mismatching C_f = 40 µF, (**b**) mismatching $L_f = 2$ mH, (**c**) mismatching $L_f = 4$ mH, (**d**) normal work condition.

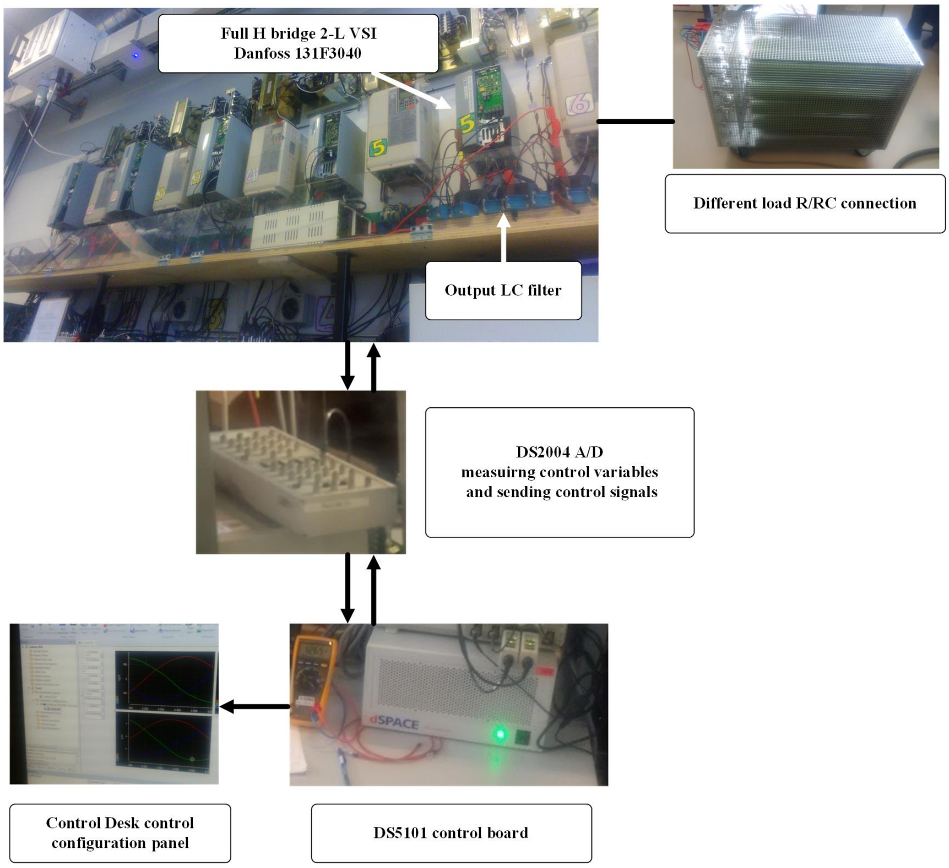

Figure 9. Laboratory experimental model stand.

7. Discussion

Both simulation and experimental validation of the presented algorithms were performed. Due to the applied algorithms, the total THD harmonic distortion was decreased to the values acceptable in standards, EN 62040-3 for both controllers. MPC- and PBC-improved controllers are good solutions for creating systems that are exposed to changing filter parameters without modifying the internal behavior of the controllers.The used configuration was 2L-VSI and full bridge at input. The main advantage of the used models configuration is the MISO solution. In many papers concerning control techniques for three-phase inverters, single- or double-loop feedback techniques were used but based only on output voltage measurements. The performed investigation proved that models composed of single-input variable are not robust enough; they work efficiently only for an exact model, e.g., deadbeat controller. That leads to a high distortion sensitivity and low-output THD reduction. Response for changes of current must be taken into account. The advantage of the solution is the faster output response. Although the used MPK-made capacitors have very small value of ESR, lack of measuring of the output current and filter current decreases the output voltage harmonic reduction. In this paper, the most efficient configuration was assumed based on [21]. Only two-level regulated VSI provides good output quality with no problem with zero crossing and less dependency on the modulation index. Apart from improved controllers, the THD_v fulfills the standards designated for UPS, even for a mismatched parameters case.

8. Conclusions

In the paper, it was proved that the enhanced MISO version of the classical PBC and MPC are the efficient control techniques for UPS standalone devices exposed for parameter changes. The examined system worked in a robust way in the range of the 12.8 kHz switching frequency. Even though each of the systems use similar input variables control, they are characterized by different abilities. It comes from the fact that MPC uses prediction of the variables' states and signals, while PBC is based on energy shaping together with the reference measurements. What could be observed during simulations is that the MPC controller kept working with constantly low THD distortion, which was not the case for the PBC. On the other hand, the PBC controller seemed to work slightly quieter due to the constant frequency. Another conclusion is that MPC was characterized by faster time response for at least one period T_s, due to lack of the modulator on the input of the device. Additionally, it was shown that both the systems are sensible for downgrading the L_f and C_f filter parameters. Finally both controllers, due to their modification and number of the input tracking variables, are proper solutions when mismatching output LC parameters are provided. They maintain low output distortion THD_v, below 8% for all cases and 1% for normal condition. Despite increasing the value of THD_v in case of downgrading the inductor value, the system fulfills requirements for the UPS inverters. Control functions can be directly implemented on a digital microprocessor or using laboratory equipment similar to that presented in the paper. In the future, the investigations could be expanded for the inverters working with different filter types, e.g., LCL, and could focus on the manufacturer's materials' parameter values accuracy evaluation.

Author Contributions: Conceptualization, Ł.D. and M.A.; methodology, Ł.D., Z.R. and M.A.; software, Ł.D. and M.A.; validation, Ł.D., M.A. and Z.R.; formal analysis, Ł.D. and M.A.; investigation, Ł.D. and M.A.; resources, Ł.D. and M.A.; data curation, Ł.D. and M.A.; writing—original draft preparation, Ł.D. and M.A.; writing—review and editing, Ł.D., M.A. and P.D.; visualization, M.A. and P.D.; supervision, Z.R. and P.D.; project administration, Ł.D. and M.A.; funding acquisition, Ł.D. and Z.R. All authors have read and agreed to the published version of the manuscript.

Funding: This work was partly supported by the Polish Ministry of Science and Higher Education funding for statutory activities.

Institutional Review Board Statement: Not applicable.

Informed Consent Statement: Not applicable.

Data Availability Statement: Not applicable.

Conflicts of Interest: The authors declare no conflict of interest. The funders had no role in the design of the study; in the collection, analyses, or interpretation of data; in the writing of the manuscript, or in the decision to publish the results.

References

1. Ortega, R.; Loria Perez, J.A.; Nicklasson, P.J.; Sira-Ramirez, H. *Passivity-Based Control of Euler-Lagrange Systems: Mechanical, Electrical and Electromechanical Applications*; Springer: London, UK, 2013.
2. Blaabjerg, F. (Ed.) *Control of Power Electronic Converters and Systems*; Academic Press: London, UK, 2018.
3. Rymarski, Z.; Bernacki, K. Different approaches to modelling single-phase voltage source inverters for uninterruptible power supply systems. *IET Power Electron.* **2016**, *9*, 1513–1520. [CrossRef]
4. Padmanaban, S.; Sharmeela, C.; Holm-Nielsen, J.B.; Sivaraman, P. *Power Quality in Modern Power Systems*; Academic Press: Cambridge, MA, USA, 2021.
5. Mattavelli, P. An Improved Deadbeat Control for UPS Using Disturbance Observers. *IEEE Trans. Ind. Electron.* **2005**, *52*, 206–212. [CrossRef]
6. Monje, C.A. *Fractional-Order Systems and Control: Fundamentals and Applications*; Advances in Industrial Control; Springer: London, UK, 2010.
7. Rodriguez, J.; Cortes, P. *Predictive Control of Power Converters and Electrical Drives: Rodriguez/Predictive Control of Power Converters and Electrical Drives*; John Wiley & Sons, Ltd.: Chichester, UK, 2012. [CrossRef]
8. Rymarski, Z. Design method of a 3-phase VSI for UPS systems. In Proceedings of the 2008 International Conference on Signals and Electronic Systems, Krakow, Poland, 14–17 September 2008. [CrossRef]
9. Rymarski, Z.; Bernacki, K.; Dyga, L. Measuring the power conversion losses in voltage source inverters. *AEU—Int. J. Electron. Commun.* **2020**, *124*, 153359. [CrossRef]
10. Gholami-Khesht, H.; Davari, P.; Blaabjerg, F. An Adaptive Model Predictive Voltage Control for LC-Filtered Voltage Source Inverters. *Appl. Sci.* **2021**, *11*, 704. [CrossRef]
11. *IEC 62040-3:2021*; Uninterruptible Power Systems (UPS)—Part 3: Method of Specifying the Performance and Test Requirements. IEC: Geneva, Switzerland, 2021.

12. *IEC 61000-2-2:2003*; Electromagnetic Compatibility (EMC)—Part 2-2: Environment—Compatibility Levels for Low-Frequency Conducted Disturbances and Signalling in Public Low-Voltage Power Supply Systems. IEC: Geneva, Switzerland 2003.
13. *IEEE 519-2014*; IEEE Recommended Practice and Requirements for Harmonic Control in Electric Power Systems. IEEE: Piscataway, NJ, USA, 2014.
14. Alhasheem, M.; Dragicevic, T.; Rivera, M.; Blaabjerg, F. Losses evaluation for a two-level three-phase stand-alone voltage source converter using model predictive control. In Proceedings of the 2017 IEEE Southern Power Electronics Conference (SPEC), Puerto Varas, Chile, 4–7 December 2017; pp. 1–6. [CrossRef]
15. Dragicevic, T.; Alhasheem, M.; Lu, M.; Blaabjerg, F. Improved model predictive control for high voltage quality in microgrid applications. In Proceedings of the 2017 IEEE Energy Conversion Congress and Exposition (ECCE), Cincinnati, OH, USA, 1–5 October 2017; pp. 4475–4480. [CrossRef]
16. Rymarski, Z.; Bernacki, K.; Dyga, Ł.; Davari, P. Passivity-Based Control Design Methodology for UPS Systems. *Energies* **2019**, *12*, 4301. [CrossRef]
17. Kouro, S.; Cortes, P.; Vargas, R.; Ammann, U.; Rodriguez, J. Model Predictive Control—A Simple and Powerful Method to Control Power Converters. *IEEE Trans. Ind. Electron.* **2009**, *56*, 1826–1838. [CrossRef]
18. Ortega, R.; García-Canseco, E. Interconnection and Damping Assignment Passivity-Based Control: A Survey. *Eur. J. Control* **2004**, *10*, 432–450. [CrossRef]
19. Ortega, R.; van der Schaft, A.; Maschke, B.; Escobar, G. Interconnection and damping assignment passivity-based control of port-controlled Hamiltonian systems. *Automatica* **2002**, *38*, 585–596. [CrossRef]
20. Zhang, M.; Borja, P.; Ortega, R.; Liu, Z.; Su, H. PID Passivity-Based Control of Port-Hamiltonian Systems. *IEEE Trans. Autom. Control* **2018**, *63*, 1032–1044. [CrossRef]
21. Rymarski, Z.; Bernacki, K. Technical Limits of Passivity-Based Control Gains for a Single-Phase Voltage Source Inverter. *Energies* **2021**, *14*, 4560. [CrossRef]
22. Serra, F.M.; De Angelo, C.H.; Forchetti, D.G. IDA-PBC control of a DC–AC converter for sinusoidal three-phase voltage generation. *Int. J. Electron.* **2017**, *104*, 93–110. [CrossRef]
23. Vu, N.T.; Lefèvre, L. A connection between optimal control and IDA-PBC design. *IFAC-PapersOnLine* **2018**, *51*, 205–210. [CrossRef]
24. Rymarski, Z.; Bernacki, K.; Dyga, L. A Control for an Unbalanced 3-Phase Load in UPS Systems. *Elektron. Ir Elektrotechnika* **2018**, *24*, 27–31. [CrossRef]
25. Komurcugil, H. Improved passivity-based control method and its robustness analysis for single-phase uninterruptible power supply inverters. *IET Power Electron.* **2015**, *8*, 1558–1570. [CrossRef]
26. Cortes, P.; Rodriguez, J.; Vazquez, S.; Franquelo, L.G. Predictive control of a three-phase UPS inverter using two steps prediction horizon. In Proceedings of the 2010 IEEE International Conference on Industrial Technology, Via del Mar, Chile, 14–17 March 2010; pp. 1283–1288. [CrossRef]
27. Loh, P.; Holmes, D. Analysis of Multiloop Control Strategies for LC/CL/LCL-Filtered Voltage-Source and Current-Source Inverters. *IEEE Trans. Ind. Appl.* **2005**, *41*, 644–654. [CrossRef]
28. Buso, S.; Fasolo, S.; Mattavelli, P. Uninterruptible power supply multiloop control employing digital predictive voltage and current regulators. *IEEE Trans. Ind. Appl.* **2001**, *37*, 1846–1854. [CrossRef]
29. Rodriguez, J.; Pontt, J.; Silva, C.A.; Correa, P.; Lezana, P.; Cortes, P.; Ammann, U. Predictive Current Control of a Voltage Source Inverter. *IEEE Trans. Ind. Electron.* **2007**, *54*, 495–503. [CrossRef]
30. Alhasheem, M.; Blaabjerg, F.; Davari, P. Performance Assessment of Grid Forming Converters Using Different Finite Control Set Model Predictive Control (FCS-MPC) Algorithms. *Appl. Sci.* **2019**, *9*, 3513. [CrossRef]
31. Vazquez, S.; Rodriguez, J.; Rivera, M.; Franquelo, L.G.; Norambuena, M. Model Predictive Control for Power Converters and Drives: Advances and Trends. *IEEE Trans. Ind. Electron.* **2017**, *64*, 935–947. [CrossRef]